

## Geology

### Mid-crustal detachment and ramp faulting in the Markham Valley, Papua New Guinea

C. Stevens, R. McCaffrey, E. A. Silver, Z. Sombo, P. English and J. van der Kevie

*Geology* 1998;26;847-850

doi: 10.1130/0091-7613(1998)026<0847:MCDARF>2.3.CO;2

---

**Email alerting services** click [www.gsapubs.org/cgi/alerts](http://www.gsapubs.org/cgi/alerts) to receive free e-mail alerts when new articles cite this article

**Subscribe** click [www.gsapubs.org/subscriptions/](http://www.gsapubs.org/subscriptions/) to subscribe to *Geology*

**Permission request** click <http://www.geosociety.org/pubs/copyrt.htm#gsa> to contact GSA

Copyright not claimed on content prepared wholly by U.S. government employees within scope of their employment. Individual scientists are hereby granted permission, without fees or further requests to GSA, to use a single figure, a single table, and/or a brief paragraph of text in subsequent works and to make unlimited copies of items in GSA's journals for noncommercial use in classrooms to further education and science. This file may not be posted to any Web site, but authors may post the abstracts only of their articles on their own or their organization's Web site providing the posting includes a reference to the article's full citation. GSA provides this and other forums for the presentation of diverse opinions and positions by scientists worldwide, regardless of their race, citizenship, gender, religion, or political viewpoint. Opinions presented in this publication do not reflect official positions of the Society.

---

#### Notes

# Mid-crustal detachment and ramp faulting in the Markham Valley, Papua New Guinea

C. Stevens }  
 R. McCaffrey } Department of Earth and Environmental Sciences, Rensselaer Polytechnic Institute, Troy, New York 12180  
 E. A. Silver } Earth Sciences Department, University of California, Santa Cruz, California 95060  
 Z. Sombo } Department of Surveying and Land Studies, University of Technology, Lae, Papua New Guinea  
 P. English }  
 J. van der Kevie } National Mapping Bureau, Boroko, Papua New Guinea

## ABSTRACT

Earthquakes and geodetic evidence reveal the presence of a low-angle, mid-crustal detachment fault beneath the Finisterre Range that connects to a steep ramp surfacing near the Ramu-Markham Valley of Papua New Guinea. Waveforms of three large ( $M_w$  6.3 to 6.9) thrust earthquakes that occurred in October 1993 beneath the Finisterre Range 10 to 30 km north of the valley reveal  $15^\circ$  north-dipping thrusts at about 20 km depth. Global Positioning System measurements show up to 20 cm of coseismic slip occurred across the valley, requiring that the active fault extend to within a few hundred meters of the Earth's surface beneath the Markham Valley. Together, these data imply that a gently north-dipping thrust fault in the middle or lower crust beneath the Finisterre Range steepens and shallows southward, forming a ramp fault beneath the north side of the Markham Valley. Waveforms indicate that both the ramp and detachment fault were active during at least one of the earthquakes. While the seismic potential of mid-crustal detachments elsewhere is debated, in Papua New Guinea the detachment fault shows the capability of producing large earthquakes.

## INTRODUCTION

Fault-bend fold geometries are found in fold-and-thrust belts worldwide (Suppe, 1985). In regions such as the Transverse Ranges and the Los Angeles, Ventura, and Santa Barbara basins, geologic and geophysical evidence suggests that seismically active ramp structures connect to

low-angle, mid-crustal regional detachments (Namson and Davis, 1988; Davis et al., 1989; Shaw and Suppe, 1994). The seismically inactive detachments are assumed to be near the base of the ramp seismicity, typically at 10–15 km depth. Yeats (1993) questioned the existence of these low-angle detachments and suggested as an alter-

native that the steep ramp faults continue through the lower crust as ductile shear zones. Destructive earthquakes are known to occur on the ramp structures, for example the 1971  $M_w$  = 6.6 San Fernando (Whitcomb et al., 1973), the 1987  $M_L$  = 5.9 Whittier Narrows (Namson and Davis, 1988), and the 1994  $M_w$  = 6.7 Northridge earthquakes. Namson and Davis (1988) concluded that in these fault systems the ramp structures have a higher earthquake potential than the detachments. Here we present evidence from Papua New Guinea that a mid-crustal detachment fault associated with an active ramp has the capability of producing large, destructive earthquakes.

## GEODETTIC MEASUREMENTS

In northeastern New Guinea, the Australian plate is moving  $N70^\circ E$  relative to the Pacific plate at a rate of about 100 mm/yr (Fig. 1) (DeMets et al., 1994). The Ramu-Markham fault of Papua New Guinea is the suture between the Finisterre island arc terrane and Australia and takes up part of the Pacific-Australia convergence. To measure the slip rate along the Ramu-Markham fault, dis-

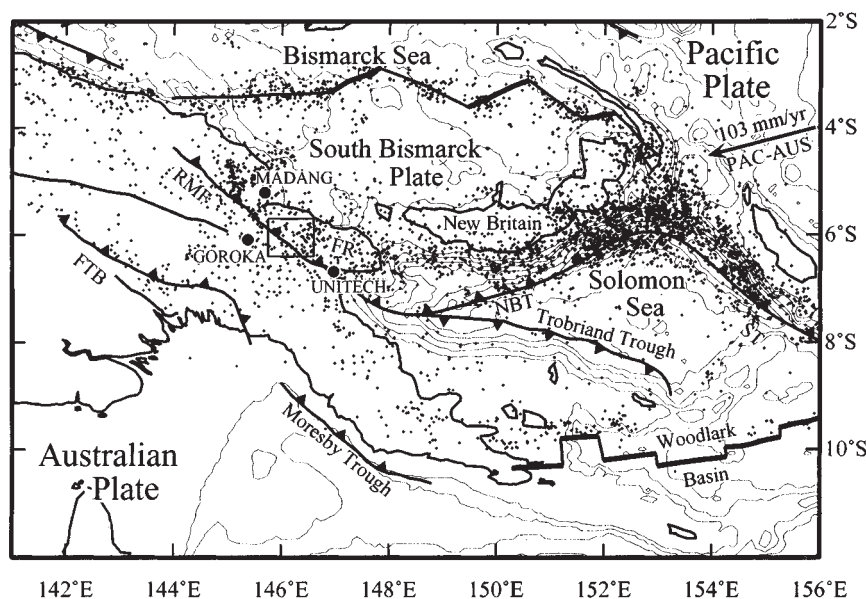


Figure 1. Tectonic map of Papua New Guinea and vicinity, adapted from Hamilton (1978). Boxed region is study area. Black circles near place names show regional Global Positioning System sites. Dots show shallow (depth <50 km) earthquake epicenters from International Seismologic Center catalog (1964–1986). FR—Finisterre Range, RMF—Ramu-Markham fault, FTB—New Guinea Highlands fold-and-thrust belt, ST—Solomon Trough, NBT—New Britain Trench. Arrow shows convergence of Pacific with Australia (PAC-AUS).

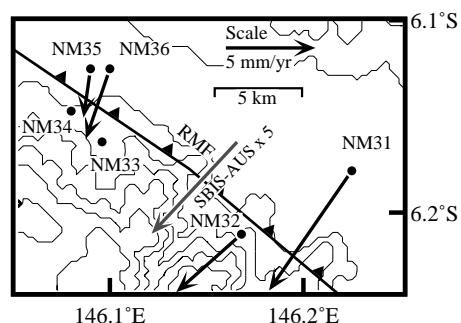
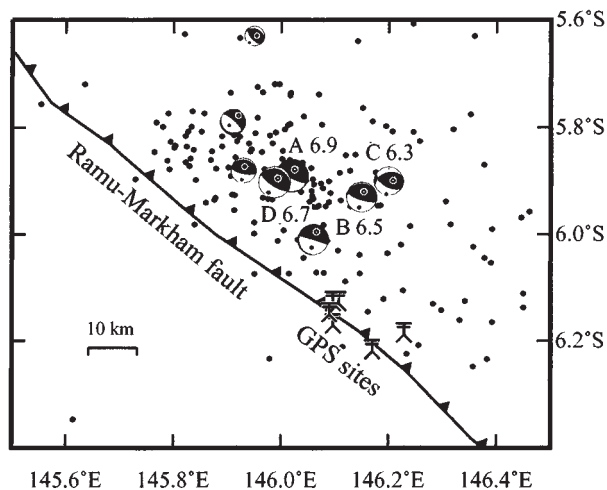


Figure 2. Comparison of 1973 and 1975 electronic distance measurements to 1993 Global Positioning System measurements shows convergence rate of about 4 mm/yr across Markham Valley. Sites NM33 and NM34 are held fixed in this analysis, which may induce false rotation of network. Vector in center shows predicted motion of the South Bismarck plate (SBIS) (hanging wall) relative to Australia (AUS) (footwall), from Tregoning et al. (1998). Length of this vector is scaled down by a factor of 5 relative to others. Location of fault is greatly uncertain. Topographic contours are 200 m and valley floor is at 400 m elevation. RMF—Ramu-Markham fault.

**Figure 3. Fault plane solutions and aftershocks of October 1993 earthquakes. Events labeled as in Table 2, and moment magnitudes are given. Also shown with smaller symbols are focal mechanisms for aftershocks with  $M_w \geq 5.5$ . Black dots are all aftershocks for a 2 month period. Three Global Positioning System (GPS) sites to northeast side of fault moved about 20 cm southwest during earthquakes.**



tances between six geodetic markers on either side of the Markham Valley (Fig. 2) were measured with electronic distance measurements in 1973 and again in 1975 (Sloane and Steed, 1976). The network spans about 5 km across the valley and 16 km along strike; thus the sites are in the foothills of the mountains bounding the valley. The electronic distance measurements showed no motion faster than 1 cm/yr during the 2 yrs. We occupied the sites in August 1993 with the Global Positioning System to estimate the 20 yr rate of motion across the valley. In January 1994, we occupied them again with the Global Positioning System to measure coseismic slip following four large thrust earthquakes that occurred north of the valley in October 1993 (Fig. 3).

Global Positioning System measurements were made using three P-code, dual-frequency Ashtech receivers (Langly, 1993). Site NM34 (Fig. 2) operated continuously. Other local sites were occupied for periods of 2 to 30 h and regional sites (Fig. 1) for 4 days. Data were processed using daily orbit solutions from Scripps Institute of Oceanography and the GAMIT/GLOBK software (King and Bock, 1996; Herring et al., 1990). The 1993 Global Positioning System baselines were converted to two-dimensional sea-level distances to compare them to published horizontal sea-level electronic distance measurement distances.

Site velocities were estimated by fixing the positions of sites NM34 and NM33 and fitting baseline length changes by least-squares. The resulting shortening across the Markham Valley of approximately 4 mm/yr (Fig. 2) is inferred to be the interseismic rate because no large earthquakes occurred in this region during the 20 year period. As expected, if the sites are close to a locked fault, the interseismic rate is considerably slower than the convergence rate between the Finisterre Range and Australia, estimated at 35 mm/yr at this location (Tregoning et al., 1998).

Horizontal coseismic displacements during the October 1993 earthquakes, determined by

comparing the August 1993 to January 1994 Global Positioning System measurements, are as large as 20 cm across the 5 km wide valley (Fig. 4, Table 1). The vertical displacements have an irregular pattern and large errors, so we do not use them for further analyses. On the hanging wall (north) side of the valley (NM31, NM35, and NM36) uplift of 42 to 87 mm occurred, whereas foot wall sites (south of the valley; sites NM32, NM33, and NM34) range from 14 mm of subsidence to 46 mm of uplift (Table 1).

#### WAVEFORM MODELING

Source parameters were estimated for two of the four largest earthquakes by formal inversion of teleseismic waveforms (events A and C; Table 2, Fig. 3). Body waves from the other two large events were in the codas of prior earthquakes and could not be modeled with our method, so the Harvard centroid moment tensor solutions are used. The waveform inversion technique minimizes the sum of the square of the residuals between observed and synthetic broadband compressional (P) and horizontal shear (SH) waveforms while estimating the centroid depth, seismic moment, rupture history (source time function), and the strike, dip, and rake angles (McCaffrey et al., 1991). The Harvard centroid moment tensor solutions use longer period seismograms (Dziewonski et al., 1981) and are less sensitive to depth and details of the rupture history than the bodywave method.

By examining the fits to waveforms while varying assumed depth, we estimate the depth of the largest event (A) at  $19 \pm 3$  km below the ground surface. Events B and D were given similar depths (24 and 20 km) and mechanisms to event A by the Harvard centroid moment tensor method. The three events have fault planes that strike parallel to the valley and indicate almost pure thrusting at a low angle (about  $15^\circ$ ) at mid-crustal depth (Table 2, Fig. 3). We infer that the north-dipping planes are the fault planes in part because of the broad distribution

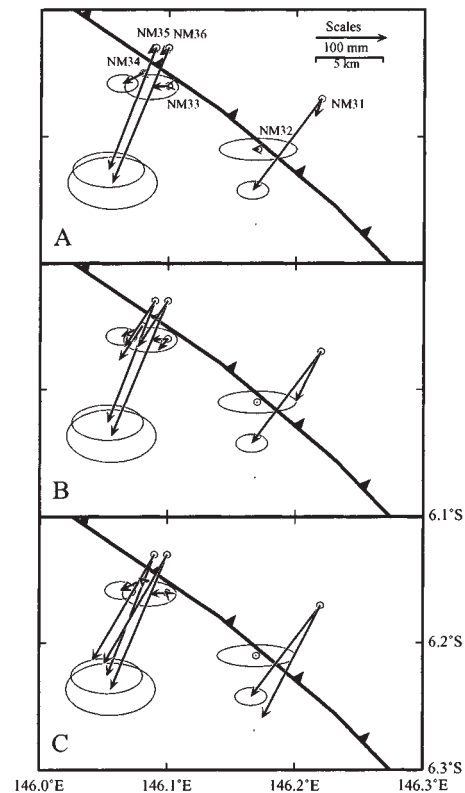


**Figure 4. Coseismic displacements and results of dislocation models indicating that rupture came close to the surface beneath Markham Valley during October 1993 earthquakes. Arrows show observed (with 95% confidence ellipses) and predicted (without ellipses) coseismic slip. Fault(s) used for dislocation modeling strike at  $298^\circ$ , have a rake of  $90^\circ$ , along-strike width of 60 km. Ramp fault starts at 0.01 km depth beneath Markham Valley, dips northeast at  $40^\circ$  (estimated from earthquakes), and connects with detachment fault at 15 km depth. Detachment fault starts at intersection with ramp fault at 15 km depth, dips northeast at  $12^\circ$  (estimated from earthquakes), and extends 50 km north of valley. Panels show results of three assumed slip distributions on detachment and ramp faults. (A) Slip on detachment fault only, dip slip = 0.67 meters; (B) 0.50 m of dip slip on detachment and 0.25 m of dip slip on the lower 8 km of the ramp; (C) 0.40 m of dip slip on the detachment and 0.21 m of dip slip on entire ramp. All models have seismic moment of about  $3.8 \times 10^{19}$  Nm.**

of aftershocks but more so because of the geodetic observations presented below.

Body-waveform inversion for event C shows a steeper dip angle ( $42^\circ$ ), a more easterly strike, and greater depth ( $29 \pm 3$  km) than the other three. We infer that this event is below the detachment. Although the fault plane of this earthquake projects to the surface of the Earth within the Markham Valley, its seismic moment was not large enough to have produced the coseismic displacements observed across the valley.

Waveforms of the largest earthquake (A) show complexity not matched by rupture of a single

fault so we allowed two events in the analysis to see if both the detachment and the ramp structures ruptured seismically (Fig. 5). Although the first 10 s of the earthquake record is matched well using a single event (Fig. 5, left), energy coming in between 10 and 20 s after the onset is matched better by a second, later rupture on a steeper fault (Fig. 5, right). The first subevent (A1) at a depth of 21 km and a dip of  $14^\circ$  is consistent with slip on the detachment fault. The second subevent (A2), that started about 11 s after the first and lasted about 5 s, has a dip of  $41^\circ$  and a depth of 9 km, consistent with rupturing of the ramp. We infer from the sequence of events that the earthquake started at depth on the detachment fault where roughly three-quarters of the moment was released, then propagated southward, rupturing up the ramp and producing the coseismic displacements observed across the Markham Valley.

## DISCUSSION

The proximity of the large October 1993 earthquakes to the geodetic network provides a unique opportunity to examine the geometry of the Ramu-Markham fault for which previous geophysical data have been inconclusive. A gently north-dipping thrust plane is expected if the Ramu-Markham fault is continuous with the New Britain trench, but no previous seismological evidence supports this. Earthquakes beneath the eastern end of the Markham Valley are both high- and low-angle thrust events. The low-angle events are too deep (20 to 25 km) to be associated with the Ramu-Markham fault as seen at the surface. The quakes may occur on a fault that extends southward to the New Guinea fold-and-thrust belt (Fig. 1) (Abers and McCaffrey, 1994). Thrust earthquakes from the west end of the valley and microseismicity studies at the east end both suggest high-angle thrusting at shallow depths (Kulig et al., 1993).

We use the earthquake locations, source parameters, seismic moment, and coseismic surface slip to constrain the fault geometry and slip using a dislocation model in a homogeneous elastic half-space (Okada, 1985). We compare observed and predicted coseismic surface displacements with the main goal of constraining how close the seismic rupture might have come to the Earth's surface beneath the valley (Fig. 4). The earthquakes were located about 30 km north of the valley on a gently-dipping fault plane at 20 km depth. Models with slip only on the low-angle detachment fault predict far too little shortening across the valley (Fig. 4A). Slip on the detachment and halfway up the ramp fault toward the valley produces more, but still not enough, coseismic slip (Fig. 4B). Slip on both the detachment and a ramp that extends nearly to the Earth's surface predicts surface displacements across the valley that agree with the observed coseismic slip (Fig. 4C). Hence, the differences in the coseismic slip on either side of the Markham Valley indicate

TABLE 1. GLOBAL POSITIONING SYSTEM SITE DISPLACEMENTS BETWEEN AUGUST 1993 AND JANUARY 1994, RELATIVE TO AUSTRALIA

Site	Latitude (°S)	Longitude (°E)	North (mm)	East (mm)	Up (mm)
NM31	-6.1786	146.2271	-159 ± 12	-95 ± 22	42 ± 42
NM32	-6.2116	146.1694	-29 ± 15	2 ± 55	0 ± 62
NM33	-6.1640	146.0966	-31 ± 17	-23 ± 37	46 ± 78
NM34	-6.1478	146.0812	-44 ± 12	-28 ± 22	-14 ± 34
NM35	-6.1252	146.0911	-201 ± 25	-64 ± 50	87 ± 106
NM36	-6.1257	146.1012	-220 ± 37	-77 ± 62	68 ± 96

Note: Uncertainties are at 2-sigma level.

TABLE 2. SOURCE PARAMETERS FOR OCTOBER 1993 EARTHQUAKES

Event	Date, Origin time	Strike (°)	Dip (°)	Rake (°)	Depth (km)	Moment ( $\times 10^{18}$ N·m)
A	Oct. 13, 1993, 0206	310 ± 4	11 ± 3	103 ± 4	19 ± 3 (15)	14.0 ± 0.7
A1	Oct. 13, 1993, 0206	310*	14 ± 3	105 ± 4	21 ± 3	7.7 ± 0.6
A2	Oct. 13, 1993, 0206	310*	41 ± 3	115 ± 9	9 ± 3	2.5 ± 0.9
B	Oct. 13, 1993, 0307	(272)	(11)	(75)	(24)	(7.2)
C	Oct. 16, 1993, 0305	255 ± 9	42 ± 3	54 ± 4	29 ± 3 (33)	2.4 ± 0.2
D	Oct. 25, 1993, 1027	(291)	(20)	(79)	(20)	(12.1)

Note: Uncertainties in depths based on waveform modeling following McCaffrey (1988). Harvard centroid moment tensor solution parameters are given in parentheses. A1 and A2 are subevents for event A.

\*Strikes of the subevents were fixed at  $310^\circ$ .

that the fault rupture came to within a few hundred meters of the Earth's surface. This finding is consistent with our inference from the waveforms of event A that the ramp also ruptured seismically. The seismic moment necessary to match the geodetic displacements ( $M_o = 3.8 \times 10^{19}$  Nm) suggests that the observed slip was probably the result of at least the two largest events (A and D). The model that fits the observed coseismic slip (Fig. 4C) has about 2/3 of the total seismic moment release on the detachment fault and the remaining 1/3 on the ramp, consistent with our inferences from waveform analysis.

Our interpretation of the Ramu-Markham fault (Fig. 6) is that a gently-dipping, middle to lower crust, seismogenic detachment fault connects to a steeper ramp that comes close to the Earth's surface beneath the Markham Valley. This interpretation is supported by the following: (1) Mainshock and aftershock epicenters determined from P-wave arrival times are almost exclusively north of the Markham Valley, indicating that the detachment did not rupture south of the valley (Fig. 3). Landslides are also concentrated on the north side of the valley. (2) Depths of the thrust earthquakes beneath the Finisterre Range are

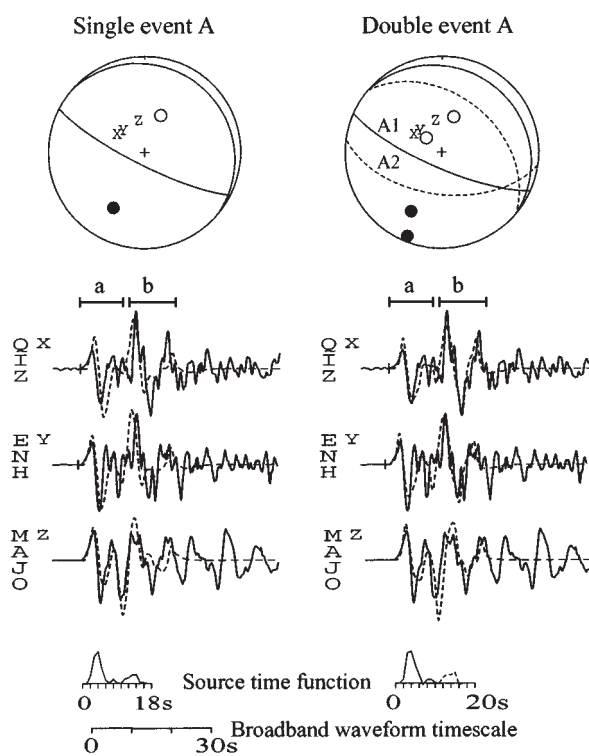
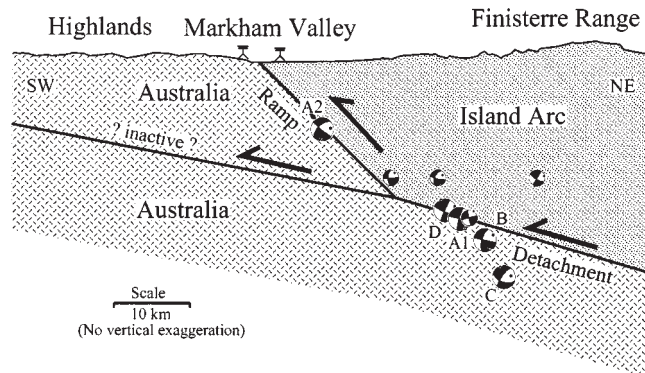


Figure 5. Fault plane solutions and broadband waveforms for earthquake A. Solutions are based on more waveforms than displayed. Solid lines are observed and dashed lines are calculated waveforms. Source parameters estimated by least-squares are listed in Table 2. Left: The first 10 s of energy in each waveform (denoted by "a") is matched well by using single, low-angle thrust mechanism, but energy coming in between 10 and 20 s (denoted by "b") is not. Right: Match to later energy is improved by including a steeper rupture that we infer to be on ramp starting about 11 s. Mechanism and source time function of second event are shown by dashed lines in beachball and on source time function axis. Dots in lower hemisphere plots at top show P axes and circles show T axes. Take-off angles for the seismograms are denoted by the X, Y, and Z in focal sphere. Source structure for generating seismograms is half-space with  $v_p = 6.5$  km/s,  $v_s = 3.7$  km/s, and density =  $2800$  kg/m<sup>3</sup>.

**Figure 6. Interpretive north-east-southwest cross section of Markham Valley region. Earthquakes reveal thrust faulting at ~20 km depth beneath Finisterre Range on detachment fault plane that dips northeast at ~15°. High coseismic strain across Markham Valley indicates that fault rupture came close to surface of Earth under valley. Hence, we suggest that low-angle detachment connects to steep ramp north of valley. Side-hemisphere focal mechanisms for earthquakes are plotted (separate subevents are shown for event A). Event A2 is inferred to be on ramp due to its steep dip and shallower depth but its epicenter is not constrained. Smaller focal mechanisms are for other aftershocks with  $M_w > 5.5$  taken from the Harvard centroid-moment tensor catalog.**



between 19 and 30 km. Three with depths of 19 to 24 km have north-dipping fault planes that dip at ~15°. (3) Up to 20 cm of differential coseismic slip occurred across the valley. Much smaller coseismic slip differences are expected if the rupture plane continued at a shallow angle southward or, or stopped at depth below, the Markham Valley. (4) The largest earthquake (A), with 40% of the total moment in the series of earthquakes, is matched better as a double event, with a gently-dipping mid-crustal event followed by high-angle slip at shallower depths.

The coseismic slip, interseismic slip rate, and plate convergence rate together suggest that the future seismic potential of the Ramu-Markham fault is significant. The convergence rate is about 35 mm/yr (Tregoning et al., 1998) and the measured aseismic slip rate at the fault in the 20 years prior to the 1993 earthquakes was no more than 5 mm/yr, indicating that the slip deficit was building at a rate of about 3 cm/yr. Hence, the coseismic slip of 20 cm during the 1993 earthquake sequence accounts for only 7 yr of convergence. No other large earthquakes have occurred on the Ramu-Markham fault during the past 40 years. Accordingly, at the longitude of the geodetic network, there is now at least a 1 m horizontal slip deficit on the fault. This deficit, if released all at once, will result in an earthquake of greater than magnitude 7.

The crustal thickness of the 4-km-high Finisterre Range is unknown, but we assume that it was originally 20 km or greater based on comparison to other island arcs. If so, the detachment at 20 km depth occurs in the middle to lower crust and does not emplace mantle rocks of the island arc on the Australian continent (Fig. 6). The affinity of the footwall rocks of the detachment underlying the high peaks of the Finisterres is unknown, but Australian rocks, which crop out on the south side of the valley, likely extend below the Finisterres some distance north of the Markham Valley.

During the 1993 Papua New Guinea earthquake sequence, both the detachment and ramp structures appeared to rupture seismically. In California, ramp-detachment thrust systems similar to the Ramu-Markham fault tend to produce large earthquakes only on the steep ramp structures, while the detachments remain aseismic (Namson and Davis, 1988; Davis et al., 1989; Shaw and Suppe, 1994). In Papua New Guinea, the detachment is seismically active and has the capability of producing large magnitude thrust earthquakes. Understanding the Papua New Guinea system has important implications for the assessment of seismic hazards in regions where ramp-detachment thrust geometries exist.

#### ACKNOWLEDGMENTS

We thank the surveyors and students from the University of Technology in Lae and the National Mapping Bureau of Papua New Guinea for participating in the field work. Hugh Davies provided logistical support and Yehuda Bock loaned us equipment. Clark Burchfiel and Kevin Furlong provided reviews. The re-occupation of the sites in January 1994 was funded at Rensselaer Polytechnic Institute by a supplement to National Science Foundation grant EAR9114349.

#### REFERENCES CITED

- Abers, G. A., and McCaffrey, R., 1994, Active arc-continent collision: Earthquakes, gravity anomalies, and fault kinematics in the Huon-Finisterre collision zone, Papua New Guinea: *Tectonics*, v. 13, p. 227–245.
- Davis, T., Namson, J., and Yerkes, R., 1989, A cross section of the Los Angeles area: Seismically active fold and thrust belt, the 1987 Whittier Narrows earthquake, and earthquake hazard: *Journal of Geophysical Research*, v. 94, p. 9644–9664.
- DeMets, C., Gordon, R. G., Argus, D. F., and Stein, S., 1994, Effects of recent revisions to the geomagnetic reversal time scale on estimates of current plate motions: *Geophysical Research Letters*, v. 21, p. 2191–2194.

- Dziewonski, A., Chou, T.-A., and Woodhouse, J., 1981, Determination of earthquake source parameters from waveform data for studies of global and regional seismicity: *Journal of Geophysical Research*, v. 86, p. 2825–2852.
- Hamilton, W., 1978, Tectonic map of the Indonesian region: U.S. Geological Survey Map I-875-D.
- Herring, T. A., Davis, J. L., and Shapiro, I. I., 1990, Geodesy by Radio Interferometry: The application of Kalman filtering to the analysis of Very Long Baseline Interferometry data: *Journal of Geophysical Research*, v. 95, p. 12561–12581.
- King, R. W., and Bock, Y., 1996, Documentation for the GAMIT Global Positioning System analysis software, Release 9.3: Cambridge, Massachusetts: Institute of Technology.
- Kulig, C., McCaffrey, R., Abers, G. A., and Letz, H., 1993, Shallow seismicity of arc-continent collision near Lae, Papua New Guinea: *Tectonophysics*, v. 227, p. 81–93.
- Langley, R. B., 1993, The Global Positioning System Observable: *Global Positioning System World*, v. 4, p. 52–59.
- McCaffrey, R., 1988, Active tectonics of the eastern Sunda and Banda arcs: *Journal of Geophysical Research*, v. 93, p. 15163–15182.
- McCaffrey, R., Abers, G. A., and Zwick, P., 1991, Inversion of teleseismic body waves: IASPEI Software Library, v. 3: Menlo Park, California, International Association of Seismology Physics Earth Interior.
- Namson, J., and Davis, T., 1988, Structural transect of the western Transverse Ranges, California: Implications for lithospheric kinematics and seismic risk evaluation: *Geology*, v. 16, p. 675–679.
- Okada, Y., 1985, Surface deformation due to shear tensile faults in a half-space: *Seismological Society of America Bulletin*, p. 1135–1154.
- Shaw, J. H., and Suppe, J., 1994, Active faulting and growth folding in the eastern Santa Barbara Channel, California: *Geologic Society of America Bulletin*, v. 106, p. 607–626.
- Sloan, B. J., and Steed, J. B., 1976, Crustal movement survey, Markham Valley–Papua New Guinea: Canberra, Department of National Resources, Division of National Mapping, Technical Report 23.
- Suppe, J., 1985, *Principles of structural geology*: Englewood Cliffs, New Jersey, Prentice-Hall, 537 p.
- Tregoning, P., Lambeck, K., Stolz, A., Morgan, P., McClusky, S., van der Beek, P., McQueen, H., Jackson, R., Little, R. P., Laing, A., and Murphy, B., 1998, Estimation of current plate motions in Papua New Guinea from Global Positioning System measurements: *Journal of Geophysical Research*, v. 103, p. 12181–12203.
- Whitcomb, J., Allen, C. R., Garmany, J. D., and Hileman, J. A., 1973, San Fernando earthquake series, 1971: Focal mechanisms and tectonics: *Reviews of Geophysics*, v. 11, p. 693–730.
- Yeats, R., 1993, Converging more slowly: *Nature*, v. 366, p. 299–301.

Manuscript received January 26, 1998

Revised manuscript received June 2, 1998

Manuscript accepted June 15, 1998